

TextureCrop: Enhancing Synthetic Image Detection through Texture-based Cropping

Despina Konstantinidou, Christos Koutlis, and Symeon Papadopoulos

CERTH - ITI, Thessaloniki, Greece

dekonstantinidou@iti.gr, ckoutlis@iti.gr, papadop@iti.gr

Abstract. Generative AI technologies produce hyper-realistic imagery that can be used for nefarious purposes such as producing misleading or harmful content, among others. This makes Synthetic Image Detection (SID) an essential tool for defending against AI-generated harmful content. Current SID methods typically resize input images to a fixed resolution or perform center-cropping due to computational concerns, leading to challenges in effectively detecting artifacts in high-resolution images. To this end, we propose TextureCrop, a novel image pre-processing technique. By focusing on high-frequency image parts where generation artifacts are prevalent, TextureCrop effectively enhances SID accuracy while maintaining manageable memory requirements. Experimental results demonstrate a consistent improvement in AUC across various detectors by 5.7% compared to center cropping and by 14% compared to resizing, across high-resolution images from the Forensynths and Synthbuster datasets.

Keywords: synthetic image detection, AI-generated image detection, pre-processing, texture-based image cropping

1 Introduction

In recent years, the generation of synthetic media has seen intense research and significant advancements, with numerous novel methods emerging in this field [14, 17, 25, 49, 51, 53]. Generative Adversarial Networks (GANs) [20] and Diffusion models [23] have revolutionized the field of synthetic image generation by enabling the creation of images as well as the modification of attributes in existing images. While these technologies offer immense creative potential, they also present serious risks for misuse, such as spreading fake news and misinformation, facilitating impersonation and fraudulent activities and influencing political narratives. The quality of generated images has reached a level where even the most careful observers can be deceived [35], posing a significant challenge for the majority of Internet users. Moreover, the diversity of fake image sources complicates the detection process, necessitating the development of robust and universal detection methods.

Researchers have recently dedicated significant effort to developing solutions to address this issue. Synthetic Image Detection (SID) is typically performed

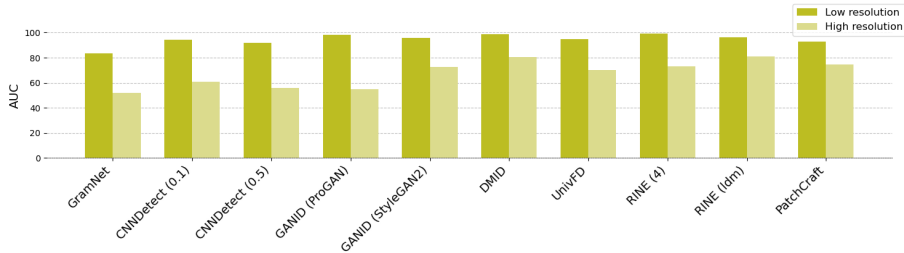


Fig. 1: Performance (AUC) of detection methods on low and high resolution images from Forensynths [50] and Synthbuster [3] datasets.

based on either image-(i.e. intensity values) or frequency-based features. Some methods apply extensive data augmentation [8, 21, 50] in order to improve generalization, while others exploit the traces left by the generation process [19, 26, 42]. Recently, numerous emerging methods [2, 11, 33, 39, 48] involve using features extracted by foundational models like CLIP [43], which has shown remarkable effectiveness in distinguishing between real and generated images.

High-resolution images are particularly relevant in the field because they often represent the higher quality and detail required for various applications, including those involving synthetic images shared online. However, limited research has been conducted on such images. With the advancement of generative AI models, there has been a significant increase in the generation of high-resolution images. Unlike older models that primarily produced lower resolution images, contemporary generative AI tools are now capable of producing high-resolution images that are widely shared across the Internet. Most state-of-the-art detection methods exhibit significant performance drops when applied to images like these, as shown in Figure 1.

The high- and low-resolution images tested in our study were derived from the same datasets as the low-resolution images and were generated using a consistent process, ensuring their similarity. Therefore, the observed performance drop can primarily be attributed to their higher resolution. This challenge arises because the majority of state-of-the-art detectors are trained using substantially smaller images (in most cases 256×256 pixels). Typically, these detectors adapt images to fixed input layers using resizing or center cropping. However, resizing entails image resampling and interpolation, which may erase the subtle high-frequency traces left by the generation process [10] (see Figure 2a) and center cropping an image to a fraction of its original size can lead to a significant loss of information (see Figure 2b). When detectors are trained and evaluated on small images, resizing or cropping has very little effect on their performance since fewer high-frequency traces are lost, but when



Fig. 2: Example of the crops created by using resizing (a), center cropping (b), slide cropping (c) and texture cropping (d).

dealing with images of higher resolution, this effect is much more pronounced.

To address this issue, we conduct an extensive investigation of pre-processing techniques during inference and introduce TextureCrop, a novel approach that targets high-frequency components, which encapsulate fine details and textures crucial for distinguishing synthetic from real images. The proposed method, leverages a sliding window technique to systematically analyze image patches. It selectively retains patches exhibiting significant texture information while discarding those that do not. Our experimental results on high-resolution images demonstrate substantial improvements in detection metrics: an increase in balanced accuracy ranging from 1.85% to 11.06% compared to the established pre-processing methods, an improvement in area under the ROC curve ranging from 2.11% to 17.07%, and an enhancement in average precision ranging from 4.57% to 13.96%.

Our main contributions can be summarized as follows:

1. We introduce TextureCrop, an innovative image pre-processing method aimed at enhancing the detection of high-resolution synthetic images by focusing on high-frequency texture components.
2. We conduct a comprehensive analysis of various pre-processing techniques applied to high-resolution images, exploring their impacts on detection performance. Our findings demonstrate that TextureCrop consistently outperforms existing pre-processing approaches across various detectors.
3. We present a detailed ablation study to fine-tune the parameters of the proposed TextureCrop method and the aggregation of results.

2 Related Work

2.1 Synthetic image generation

Over the past few years, image generation models have gained considerable attention due to their ability to create high-quality images that closely resemble real ones. Most of the preliminary research has centered on images generated by Generative Adversarial Networks (GAN), as these architectures

were introduced first and have dominated the field. Since the introduction of GANs, numerous variants have been developed [5, 9, 29, 31, 37, 40, 44, 56]. StyleGAN [31] for instance, as well as its subsequent versions StyleGAN2 [32] and StyleGAN3 [30], introduced a style - based architecture with adaptive instance normalization, enabling fine - grained control over image attributes and improved disentanglement of the latent space for generating highly realistic and diverse images.

More recently, diffusion models [1, 4, 36, 38, 41, 45–47] have emerged as an alternative approach to image generation. Notable among these are text-to-image generation models like DALL-E 2 [45] and DALL-E 3 [4]. DALL-E 2 employs a transformer - based encoder to convert textual descriptions into a latent space representation, which is then decoded using an auto-regressive model to generate images. DALL-E 3 builds upon its predecessor with improved training methods and dataset utilization. Stable diffusion models, such as Stable Diffusion 2 [47] and Stable Diffusion XL [41], utilize latent representations from training data to progressively add noise to images. Firefly [1], developed by Adobe, is another notable addition to text-to-image generation tools.

In addition to GANs and diffusion models, there are low-level vision generative models focused on pixel-level manipulation and enhancement. For example, the Second Order Attention Network (SAN) [15] enhances single image super-resolution using second - order attention mechanisms and recursive feature networks. Similarly, the Seeing In The Dark (SITD) [7] model employs fully convolutional networks to simulate long - exposure photography from low-light conditions based on short - exposure raw camera input.

2.2 Synthetic image detection

The development of robust deep learning - based detectors for synthetic images has been a major focus of recent research. Training set diversity has been found to help generalize to unseen architectures, as shown in [50], where a simple pre-trained ResNet50 [22] is trained on 20 different object classes of real images from LSUN [54] and ProGAN [29] images. It has also been found important to avoid resizing, as observed in [10], as it may erase the artifacts left by the generative model. In order to preserve these subtle high-frequency traces, some methods propose working on local patches [6], as well as analyzing both local and global features [28]. Another method proposes avoiding downsampling steps in the first layers of the network [10, 21].

Recently, there have been efforts to leverage the capabilities of pre-trained vision - language models (VLMs) for synthetic image detection purposes [2, 11, 39, 48]. For instance, [39] uses the same training protocol as in [50], but employs a pretrained VLM, the Contrastive Language - Image Pre-Training (CLIP) model, as a feature extractor instead of training a ResNet - 50. Another method [33] proposes the extraction of features not only from the

last layer of CLIP’s image - encoder, but also from intermediate layers.

Additionally, recent works have focused on analyzing the texture characteristics of images. It has been observed in [34] that synthetic faces exhibit significantly different textures compared to real ones. Additionally, [55] highlights that texture patches contain more distinct traces left by generative models than global semantic information, while [27] demonstrates that generative models tend to focus on generating the patches with rich textures to make the images more realistic and neglect the hidden noise caused by camera capture present in simple patches.

Building upon the interest in image texture, we analyze the impact of rich and poor texture regions within images on detectors’ performance. Unlike [55], that focuses on using high-pass filters for texture classification across two branches and [27] that uses noise patterns from single patches to identify synthetic images, our approach is a pre-processing method that specifically selects regions with rich textures for processing by detectors.

3 Proposed Approach

3.1 Problem Formulation

In synthetic image detection, the goal is to determine whether an image, $I \in \mathbb{R}^{C \times W \times H}$, is generated or real, where C , H , and W denote the number of channels (in most cases 3), height and width of the image, respectively. Typically, this involves processing the image with a detection model f that outputs a SID score s , indicating the likelihood of the image being synthetic. In the traditional approach, a single image I (or a batch of images), is fed into the model f , resulting in a SID score $s \in [0, 1]$:

$$s = f(I) \tag{1}$$

This approach assumes that a resized or cropped version of an image is processed, which may result in significant loss of information that can alter the outcome of the detection. In some cases, when the image is processed as a whole, processing times and resource needs increase significantly. In our proposed approach, denoted as TextureCrop, the image I is divided into a batch of smaller texture-rich crops $\{C_i\}_{i=1}^{N_I} \in \mathbb{R}^{N_I \times C \times W^c \times H^c}$, where C_i represents the i -th crop with dimensions $C \times W^c \times H^c$, where C is the number of channels and W^c and H^c are the width and height of each crop and N_I is the number of crops generated for the image I . The number of crops depends on the texture information of each image. Then this batch of crops is processed by the same detection model f , returning a SID score s_i for each crop C_i . The final SID score s is obtained by aggregating the scores from the batch of crops with an aggregation function \mathcal{A} :

$$\{C_i\}_{i=1}^{N_I} = \text{TextureCrop}(I) \quad (2)$$

$$s_i = f(C_i), \quad \text{for } i = 1, \dots, N_I \quad (3)$$

$$s = \mathfrak{A}(\{s_i\}_{i=1}^{N_I}) \quad (4)$$

3.2 Method Overview

The proposed image cropping technique, denoted as TextureCrop, leverages the idea that generative models leave artifacts in the high-frequency components of synthetic images. It is designed to enhance synthetic image detection by excluding texture-less regions from input images. This approach expands upon previous methods in image forensics, such as [12,13,24] that prioritize processing textured regions to improve detection accuracy.

Employing a sliding window approach with user-defined window size ω and stride β , TextureCrop systematically traverses I to generate crops. Each crop is converted to grayscale, and its standard deviation (SD) of pixel intensities is computed to assess the presence of texture. Then, the method utilizes a standard deviation thresholding mechanism to filter cropped regions (see Figure 2d).

If $\sigma_i > \tau$, keep C_i ; otherwise discard, $i = 1, \dots, N_I$,

where σ_i is the standard deviation of pixel intensities of the crop C_i and τ is the threshold. The resulting cropped regions

$$\{C_i\}_{i=1}^{n_I} = \text{TextureCrop}(I, \omega, \beta, \tau), \quad n_i \leq N_i$$

are then fused using an appropriate method \mathfrak{A} , and a final prediction is generated. In cases where no suitable cropped regions meet the SD threshold τ , a default center crop of 224×224 pixels is returned. This fallback ensures that at least one cropped image is available for downstream analysis, maintaining consistency in output format.

To further explain the intuition behind our cropping method choice, we introduce SlideCrop, which is a cropping method that mirrors TextureCrop but skips the step of removing regions lacking texture. Consequently, all patches generated by the sliding window are retained in SlideCrop. Among the examined images, spanning resolutions from 1024×1024 to 6030×4032 , TextureCrop filters out almost half of the patches that SlideCrop would keep. This curation enhances performance and computational efficiency. With this slight modification, TextureCrop minimizes the number of crops processed by detectors, as can be seen in Figure 2d, reducing processing time and ensuring that only the most pertinent crops are retained for analysis, thus optimizing overall performance.

3.3 Implementation Details

TextureCrop and SlideCrop methods begin by evaluating the resolution of the input image I . If I exceeds 2048×2048 pixels then the image undergoes a center crop operation to limit its size to 2048×2048 or to its maximum possible size if the image is not square. While it is technically possible to process higher resolution images, this comes at a significant computational cost. This approach ensures more predictable runtime behavior, as the complexity of processing is directly related to the original resolution and specific parameters of the generative model. The size aligns well with the capabilities of most known generative models. Until now, only a few generative models have demonstrated the capability to generate images up to 2048×2048 resolution, making this threshold a suitable compromise for effective processing and analysis. In most cases, images with resolutions higher than 1024×1024 often result from super-resolution methods.

4 Experimental Setup

4.1 Competing Image Pre-processing Approaches for SID

Pre-processing techniques employed to prepare images for precise analysis by SID models are limited. Many contemporary detectors commonly utilize center cropping or resizing as standard pre-processing steps. Center cropping involves selecting a square or rectangular area from the center of an image, focusing on retaining key features while potentially discarding peripheral details that may also contain valuable information, leading to notable information loss in some cases. Conversely, resizing adjusts an image to a specified target size through scaling, a process that can introduce distortions and diminish fine details, particularly when altering images to significantly divergent dimensions.

More recent works, such as [33], have adopted 10-cropping for handling images of higher resolutions. This involves extracting 10 distinct crops from an image: its four corners, central region, and their horizontal flips. Each crop is then independently passed through the detection model, and predictions are combined to enhance accuracy. Moreover, our method incorporates slide-cropping as a preliminary step, involving the systematic sliding of a window across the image to extract sub-images at each position. This approach aims to capture local details comprehensively throughout the entire image, but we have refined this process in our method to limit the number of extracted sub-images while still ensuring thorough coverage and detail capture.

4.2 Datasets

We evaluated our method using high-resolution data sourced from two primary datasets: Forensynths [50] and Synthbuster [3]. After filtering out images with resolutions lower than 1024×1024 , we collected a total of 6,462 images. Among

Table 1: Forensynths [50] and Synthbuster [3] datasets after removing low resolution images.

Subset/Generative model	Dataset	Total images	Real images	Generated images	Resolutions produced by the generative model
SAN	Forensynths	20	10	10	depends on the resolution of the input image
SITD	Forensynths	360	180	180	depends on the resolution of the input image
Whichfaceisreal	Forensynths	2000	1000	1000	up to 1024×1024
DALL-E 2	Synthbuster	1000	*	1000	256×256 , 512×512 , 1024×1024
DALL-E 3	Synthbuster	1000	*	1000	1024×1024 , 1024×1792 , 1792×1024
Firefly	Synthbuster	1000	*	1000	2048×2048 , 2304×1792 , 1792×2304 , 2688×1536
Stable Diffusion 2	Synthbuster	41	*	41	512×512 , 768×768
Stable Diffusion XL	Synthbuster	41	*	41	1024×1024 , 1152×896 , 896×1152 , 1216×832 , 832×1216 , 1344×768 , 768×1344 , 1536×640 , 640×1536

* For real data, we used 1000 high-resolution images from the RAISE dataset [16].

these, 4,272 images are generated by eight different generative models, while the remaining 2,190 images are real images. This distribution is detailed in Table 1. Specifically, the Forensynths dataset includes high-resolution images generated by the SAN [15] and the SITD model [7] and faces generated by the StyleGAN [31] model available on the Whichfaceisreal website [52]. For the Synthbuster dataset, high-resolution images were generated by DALL-E 2 [45], DALL-E 3 [4], Firefly [1], Stable Diffusion 2 [47], and Stable Diffusion XL [41]. Additionally, for real data, we used 1000 uncompressed and unprocessed high-resolution images from the RAISE dataset [16]. The Forensynths dataset includes its own real data.

4.3 SID Detectors

We include the following state-of-the-art detectors in our study: GramNet [34] that leverages global image texture representations, CNNDetect [50] a ResNet50 with blurring and compression augmentation (with two different probabilities of the image being augmented: 0.1 and 0.5), GANID [21] a ResNet50 with intense augmentation that avoids down-sampling in the first layer (trained on ProGAN or StyleGAN2 data), DMID [10] which proposes the fusion of the logits of two models same as described before but one trained on GAN and the other on diffusion data, UnivFD [39] that uses linear probing on features extracted from CLIP’s ViT-L/14 image encoder [18], RINE [33] that uses the image representations extracted by intermediate layers of CLIP’s image encoder (trained on 4 object classes of ProGAN data and on Latent Diffusion Model (LDM) data and PatchCraft [55], which exploits the inter-pixel correlation contrast between rich and poor texture regions within an image.

4.4 Aggregation methods

Our method results in a large number of crops per image, creating the need for an aggregation process to consolidate the information from all the individual crops into a single prediction. To achieve this, we explore the following aggregation methods:

- **Average:** This calculates the average of the logits obtained from the crops, aiming to find a balanced representation of the predictions.
- **Majority Voting:** This involves collecting the predictions from all crops and selecting the most commonly predicted class among the crops, assuming that this is more likely to be the correct one.
- **Max:** This selects the maximum logit value among the logits obtained from all the crops, assuming that the highest logit value corresponds to the most confident prediction among the crops. However, in scenarios where a single crop produces an unusually high logit value due to random fluctuations or outliers, false positives can occur, leading to an incorrect prediction.
- **Median:** This computes the median of the logits obtained from multiple crops. By selecting the middle value in the sorted list of logits, this method aims to mitigate the influence of outliers.
- **Weighted Average:** This assigns a weight to the probability obtained from each crop and calculates the average across all crops. After partitioning the $[0,1]$ range into intervals (interval length is specified by the user, in our case it is set to 0.1 after experimentation), the method calculates the percentage of values within each interval. These percentages determine the weights assigned to each value, with higher weights assigned to values in the intervals that occur more frequently. By multiplying each value by its weight and summing the weighted values, the method effectively combines the contributions of all input data. The final fused value represents an averaged representation of the input data with greater emphasis on values that are more prevalent among the sources.

4.5 Evaluation protocol

To evaluate the performance of the proposed pre-processing technique, we compute balanced accuracy (BA), average precision (AP), and area under the ROC curve (AUC) metrics. Each of these addresses different aspects of SID performance. BA accounts for class imbalance by averaging recall across all classes. AP summarizes the precision - recall curve, which is especially useful for imbalanced datasets. AUC is also particularly valuable, because it is invariant to class distribution and provides a comprehensive measure of performance across all classification thresholds. The results presented are averages across all datasets, ensuring a robust evaluation of the method’s performance.

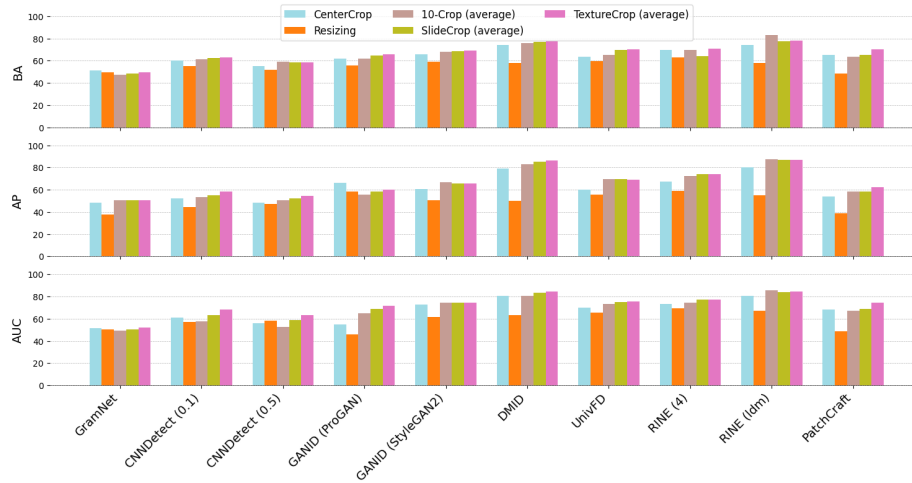


Fig. 3: Performance (BA/AP/AUC) of detection methods on high resolution images from Forensynths and Synthbuster datasets using different pre-processing methods.

5 Results

5.1 Detection Gains

In this section, we evaluate the effectiveness of the proposed texture cropping method in enhancing synthetic image detection across various deep learning models. We compare texture cropping against several standard pre-processing techniques, including center cropping, resizing, 10-cropping, and slide cropping.

On average across all detectors and datasets, the method offers a 3.13% increase in BA compared to center cropping across the 10 methods tested, along with a 5.17% increase in AP and a 5.71% increase in AUC (see Figure 3). In comparison to resizing, it demonstrates an 9.33% increase in BA, a 15.78% increase in AP and a 13.96% increase in AUC. Furthermore, it exhibits a 1.85% increase in BA compared to ten cropping along with a 2.11% increase in AP and a 4.57% increase in AUC. The results demonstrate a high degree of consistency across all datasets except for the DALL-E 3 data, which seem to perform better with resizing. Additionally, texture cropping not only outperforms slide cropping in most cases but also proves to be more computationally efficient, processing almost half the images handled by slide cropping. Consequently, this approach leads to significantly reduced processing time. These findings highlight the substantial enhancement in detection performance achieved with texture cropping across various metrics and models, while maintaining efficient processing times.

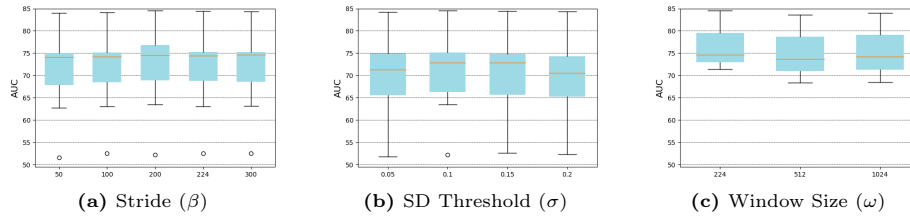


Fig. 4: Box plot of AUC distribution across detection methods for different stride parameters (a), SD thresholds (b), and window sizes (c).

5.2 Ablation Studies

In this section, we present the ablation studies conducted to fine-tune the parameters of the proposed method and the aggregation of results, and introduce a variant of the method. We explore the impact of different parameter values on the performance, ultimately determining the optimal settings for SID.

Stride (β): The stride parameter, β , controls the step size of the sliding window used in cropping the image. We experimented with strides of 50, 100, 200, 224, and 300 pixels to determine the optimal balance between computational efficiency and detection performance. Our experiments revealed that a stride of 200 pixels provides the best performance on most detection methods, as illustrated in Figure 4a. This setting offers sufficient coverage of the image while maintaining reasonable computational demands.

Standard Deviation Threshold (τ): The standard deviation threshold, τ , is crucial for filtering out texture-less regions from the cropped images. We consider 0.05, 0.1, 0.15, and 0.2 as threshold candidates. As observed in Figure 4b, a standard deviation threshold of 0.1 is ideal. This threshold effectively filters out regions with minimal texture, which are less likely to contain high-frequency artifacts introduced by generative models.

Window Size (ω): Most methods in our analysis have a set input size of 224×224 pixels, except for GANID (ProGAN and StyleGAN2) and DMID. Therefore, we tested our method with different window sizes to accommodate these variations. We set the window size parameter, ω , to 224×224 , 512×512 , and 1024×1024 pixels to determine the optimal size for capturing high-frequency artifacts while maintaining computational efficiency. Our findings indicate that a window size of 224×224 pixels provides the best results (Figure 4c).

Aggregation: Another perspective we explored involves the aggregation of the predictions across multiple image crops. Each detector model produces a logit per crop, thus to consolidate the results from multiple crops, we tested

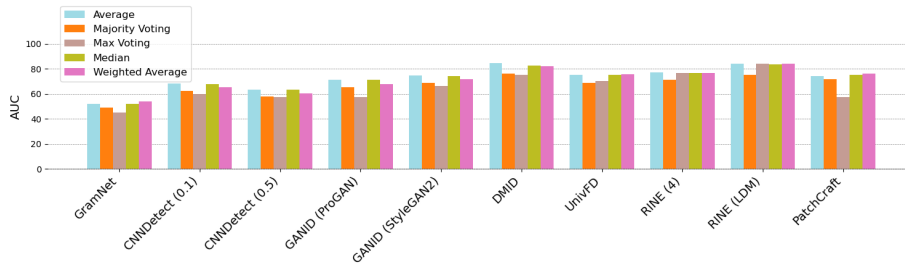


Fig. 5: Performance (AUC) of detection methods using TextureCrop with different aggregation methods.

various aggregation methods, including average, max, median, majority vote, and weighted average. The results of these tests are outlined in Figure 5. In our experimental setup, average, median and weighted average emerge as the most effective aggregation strategies, consistently delivering competitive performance across various detection methods. On the other hand, majority voting and max aggregation appear to be less effective overall, especially in scenarios where there is significant uncertainty among the crops.

Number of Crops (n): Additionally, we explored the impact of retaining a predetermined number of crops rather than applying thresholding. Our method favors thresholding because it allows for a clear cutoff point, ensuring that only the most relevant crops, as determined by our chosen metric, are retained. However, determining the optimal threshold can be challenging, as it requires complex and context-specific analysis to identify an appropriate value. Retaining a fixed number of crops also ensures consistent processing time for each image, which is crucial for scalability and efficiency in practical applications. Thus, this new variant of TextureCrop, denoted as FixedTextureCrop(I, m, p, n), selects n crops based on the metric m . The parameter p determines from which part of the distribution the crops are selected.

First, we examine the relationship between the number of crops and detection effectiveness for FixedTextureCrop($m=SD, p=top, n$), that selects the top n crops based on SD. The results of this analysis are presented in Table 2. Our analysis reveals that this method consistently achieves the highest performance metrics across various deep learning models when selecting 15 crops from the input image. By selecting a greater number of crops, the FixedTextureCrop($m=SD, p=top, n$) method captures more diverse regions of interest within the image, enhancing the model’s ability to detect high-frequency artifacts introduced by generative models. Therefore, our results emphasize the importance of considering an adequate number of crops in the design of cropping methodologies for synthetic image detection.

Table 2: Performance (BA/AP/AUC) of FixedTextureCrop(m=SD, p=top, n) method across different n parameters. Best performance is denoted with **bold**.

BA/AP/AUC	n=1	n=2	n=5	n=10	n=15
GramNet	50.19 /48.07/50.49	48.69/49.53/51.18	48.72/50.14/51.86	49.96/50.60/52.44	50.04/ 50.87 / 52.66
CNNDetect (0.1)	61.08/54.36/64.44	61.75/55.31/65.35	62.61/55.77/65.93	62.94 /56.81/67.06	62.82/ 57.27 / 68.30
CNNDetect (0.5)	61.08/53.46/64.44	61.75/53.91/65.3	62.61/54.31/65.93	62.94 /54.87/67.06	62.82/ 55.31 / 68.30
GANID (ProGAN)	64.09/56.35/67.66	64.47/56.73/68.63	63.91/57.97/69.30	64.51/59.24/70.66	65.65 / 59.84 / 71.38
GANID (StyleGAN2)	68.16/62.36/73.28	68.64/63.95/74.24	69.18/64.34/74.13	69.34 /65.15/74.11	69.11/ 65.56 / 74.60
DMID	76.82/83.13/83.13	76.59/84.21/82.79	78.40/85.11/83.77	79.11/85.91/84.20	79.14 / 86.30 / 84.52
UnivFD	62.62/57.02/66.56	63.93/59.98/68.28	66.08/63.14/70.22	67.73/65.88/72.42	69.02 / 66.85 / 73.64
RINE (4)	68.74/64.49/69.95	69.24/65.27/70.35	71.75/68.24/72.80	73.25/71.43/74.57	74.54 / 71.63 / 75.11
RINE (ldm)	72.51/77.62/79.04	72.96/81.72/80.36	75.21/83.57/81.49	75.94/85.00/82.66	76.25 / 85.50 / 82.81
PatchCraft	69.05/56.11/73.00	70.06/57.37/72.91	71.27/59.27/74.50	71.13/61.66/74.99	71.44 / 61.88 / 75.31

Image crops aggregation (parameters p and m): When it comes to selecting crops from different parts of the distribution we explored the following options: top n crops, bottom n crops and top-bottom-intermediate n crops (TBI), where we select the top $\frac{n}{3}$ crops, the bottom $\frac{n}{3}$ crops, and $\frac{n}{3}$ intermediate crops. When contrasting top and bottom crop selections based on SD, we note that the FixedTextureCrop(m=SD, p=bottom, n=15) method exhibits relatively poorer performance compared to FixedTextureCrop(m=SD, p=top, n=15). On average, FixedTextureCrop(m=SD, p=bottom, n=15) demonstrates a 6.93% decrease in BA, a 7.15% decrease in AP, and a 9.13% decrease in area under the curve. This indicates that focusing on regions with low SD may not adequately capture critical features for effective detection. The FixedTextureCrop(m=SD, p=TBI, n=15) method performs better than FixedTextureCrop(m=SD, p=bottom, n=15) but still falls short of FixedTextureCrop(m=SD, p=top, n=15). On average, it registers a 1.92% lower BA, a 2.27% lower AP, and a 4.13% lower area under the curve. These differences in performance are clearly illustrated in Figure 6a.

In addition to exploring SD as a criterion for selecting crops in our cropping method, we conducted further experimentation to assess the effectiveness of alternative approaches. Specifically, we investigated the use of entropy and autocorrelation as metrics for crop selection. Entropy measures the unpredictability or complexity of pixel values, while autocorrelation evaluates the similarity of a pixel to its neighboring pixels. Both metrics can provide insights into the texture of image regions.

The FixedTextureCrop(m, p=top, n=15) method selects the top 15 crops from the input image based on the SD, when m=SD, entropy, when m=entropy, and autocorrelation, when m=autocorrelation, of pixel intensities within each crop region. Across various models, it appears that the SD- and entropy-based methods perform similarly on average and outperform the autocorrelation-based

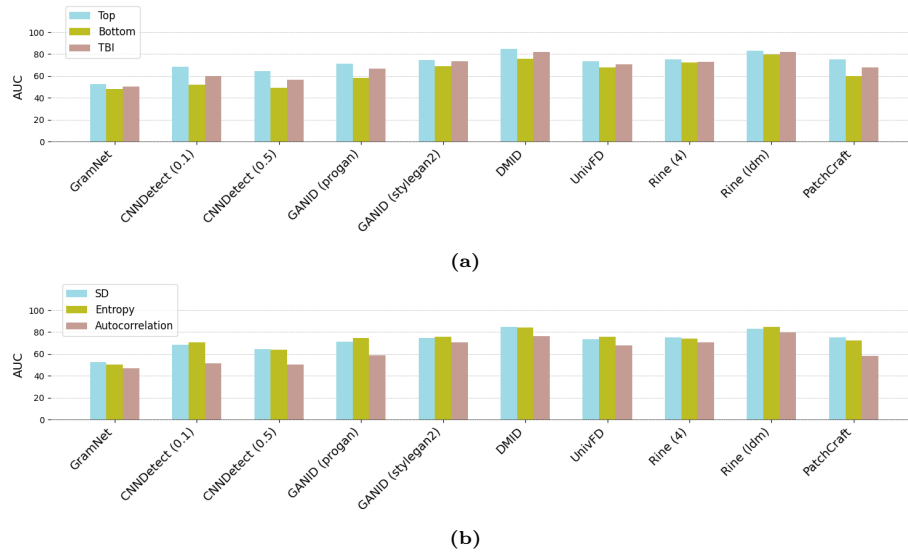


Fig. 6: Performance (AUC) of different detectors using FixedTextureCrop($m=SD$, p , $n=15$) method based on different texture selection criteria (a) and FixedTextureCrop(m , $p=top$, $n=15$) method based on different metrics for computing texture (b).

method (see Figure 6b), suggesting that utilizing SD or entropy for selecting top crops leads to superior results. Remarkably, in some cases, FixedTextureCrop method outperforms even TextureCrop, while offering the advantage of a fixed output. The choice between the two depends on the preferences of the user. TextureCrop selects an unknown number of crops for an image, as different images have different textures. In contrast, the FixedTextureCrop method offers a fixed number of crops, which may be preferable in scenarios where a fixed processing time or output size is required.

6 Conclusion

In this study, we conducted a comprehensive analysis of post-processing methods applied during inference for synthetic image detection purposes and introduced TextureCrop and FixedTextureCrop, two novel approaches that analyze texture variability for crop selection. By targeting regions of the image with high texture variability, these methods successfully capture high-frequency artifacts introduced by generative models, resulting in enhanced detection accuracy across various deep learning models. Overall, TextureCrop and FixedTextureCrop methods emerge as promising solutions for addressing the challenges associated with synthetic images and for advancing the capabilities of detection systems in accurately identifying such artifacts.

7 Acknowledgments

This work is partially funded by the Horizon 2020 European project vera.ai under grant agreement no. 101070093.

References

1. Adobe Firefly: <https://www.adobe.com/sensei/generative-ai/firefly.html> (2024)
2. Amoroso, R., Morelli, D., Cornia, M., Baraldi, L., Bimbo, A.D., Cucchiara, R.: Parents and children: Distinguishing multimodal deepfakes from natural images. arXiv preprint arXiv:2304.00500v1 (2023)
3. Bammeey, Q.: Synthbuster: Towards detection of diffusion model generated images. In: IEEE Open Journal of Signal Processing (2023)
4. Betker, J., Goh, G., Jing, L., Brooks, T., Wang, J., Li, L., Ouyang, L., Zhuang, J., Lee, J., Guo, Y., Manassra, W., Dhariwal, P., Chu, C., Jiao, Y.: <https://openai.com/dall-e-3> (2023)
5. Brock, A., Donahue, J., Simonyan, K.: Large scale gan training for high fidelity natural image synthesis. In: ICLR (2019)
6. Chai, L., Bau, D., Lim, S.N., Isola, P.: What makes fake images detectable? understanding properties that generalize. In: ECCV (2020)
7. Chen, C., Chen, Q., Xu, J., Koltun, V.: Learning to see in the dark. In: IEEE/CVF Conference on Computer Vision and Pattern Recognition (CVPR) (2020)
8. Chen, L., Zhang, Y., Song, Y., Wang, J., Liu, L.: Ost: Improving generalization of deepfake detection via one-shot test-time training. In: NeurIPS (2022)
9. Choi, Y., Choi, M., Kim, M., Ha, J.W., Kim, S., Choo, J.: Stargan: Unified generative adversarial networks for multi-domain image-to-image translation. In: CVPR (2018)
10. Corvi, R., Cozzolino, D., Zingarini, G., Poggi, G., Nagano, K., Verdoliva, L.: On the detection of synthetic images generated by diffusion models. In: ICASSP 2023-2023 IEEE International Conference on Acoustics, Speech and Signal Processing (ICASSP). pp. 1–5 (2023)
11. Cozzolino, D., Poggi, G., Corvi, R., Nießner, M., Verdoliva, L.: Raising the bar of ai-generated image detection with clip. arXiv preprint arXiv:2312.00195 (2023)
12. Cozzolino, D., Poggi, G., Verdoliva, L.: Splicebuster: A new blind image splicing detector. In: IEEE International Workshop on Information Forensics and Security (WIFS) (2015)
13. Cozzolino, D., Verdoliva, L.: Noiseprint: a cnn-based camera model fingerprint. arXiv preprint arXiv:1808.08396 (2018)
14. Croitoru, F.A., Hondru, V., Ionescu, R.T., Shah, M.: Diffusion models in vision: A survey. IEEE Transactions on Pattern Analysis and Machine Intelligence, **14** (2022)
15. Dai, T., Cai, J., Zhang, Y., Xia, S.T., Zhang, L.: Second-order attention network for single image super-resolution. In: IEEE/CVF Conference on Computer Vision and Pattern Recognition (CVPR). pp. 11065–11074 (2019)
16. Dang-Nguyen, D.T., Pasquini, C., Conotter, V., Boato, G.: Raise: a raw images dataset for digital image forensics. In: Proceedings of the 6th ACM Multimedia Systems Conference (2015)

17. Dhariwal, P., Nichol, A.: Diffusion models beat gans on image synthesis. In: *Advances in Neural Information Processing Systems* (2021)
18. Dosovitskiy, A., Beyer, L., Kolesnikov, A., Weissenborn, D., Zhai, X., Unterthiner, T., Dehghani, M., Minderer, M., Heigold, G., Gelly, S., Uszkoreit, J., Houlsby, N.: An image is worth 16x16 words: Transformers for image recognition at scale. *arXiv preprint arXiv:2010.11929* (2020)
19. Frank, J., Eisenhofer, T., Schönherr, L., Fischer, A., Kolossa, D., Holz, T.: Leveraging frequency analysis for deep fake image recognition. In: *Proceedings of the 37th International Conference on Machine Learning*, PMLR 119 (2020)
20. Goodfellow, I.J., Pouget-Abadie, J., Mirza, M., Xu, B., Warde-Farley, D., Ozair, S., Courville, A., Bengio, Y.: Generative adversarial nets. In: *Advances in Neural Information Processing Systems (NIPS)* (2014)
21. Gragnaniello, D., Cozzolino, D., Marra, F., Poggi, G., Verdoliva, L.: Are gan generated images easy to detect? a critical analysis of the state-of-the-art. In: *IEEE ICME* (2021)
22. He, K., Zhang, X., Ren, S., Sun, J.: Deep residual learning for image recognition. In: *Proceedings of the IEEE/CVF Conference on Computer Vision and Pattern Recognition* (2016)
23. Ho, J., Jain, A., Abbeel, P.: Denoising diffusion probabilistic models. In: *Advances in Neural Information Processing Systems*. vol. 33, pp. 6840–6851 (2020)
24. Iakovidou, C., Zampoglou, M., Papadopoulos, S., Kompatsiaris, Y.: Content-aware detection of jpeg grid inconsistencies for intuitive image forensics. *Journal of Visual Communication and Image Representation* (2018)
25. Jabbar, A., Li, X., Omar, B.: A survey on generative adversarial networks: Variants, applications, and training. *ACM Computing Surveys* **54**, 1–49 (2020)
26. Jeong, Y., Kim, D., Ro, Y., Choi, J.: FrepGAN: Robust deepfake detection using frequency-level perturbations. In: *AAAI* (2022)
27. Jiakuan Chen, Jieteng Yao, L.N.: A single simple patch is all you need for ai-generated image detection. *arXiv preprint arXiv:2402.01123* (2024)
28. Ju, Y., Jia, S., Ke, L., Xue, H., Nagano, K., Lyu, S.: Fusing global and local features for generalized ai-synthesized image detection. In: *IEEE ICIP* (2022)
29. Karras, T., Aila, T., Laine, S., Lehtinen, J.: Progressive growing of gans for improved quality, stability, and variation. In: *ICLR* (2018)
30. Karras, T., Aittala, M., Laine, S., Härkönen, E., Hellsten, J., Lehtinen, J., Aila, T.: Alias-free generative adversarial networks. In: *35th Conference on Neural Information Processing Systems (NeurIPS)*. (2021)
31. Karras, T., Laine, S., Aila, T.: A style-based generator architecture for generative adversarial networks. In: *CVPR* (2019)
32. Karras, T., Laine, S., Aittala, M., Hellsten, J., Lehtinen, J., Aila, T.: Analyzing and improving the image quality of styleGAN. In: *CVPR* (2020)
33. Koutlis, C., Papadopoulos, S.: Leveraging representations from intermediate encoder-blocks for synthetic image detection. *arXiv preprint arXiv:2402.1909* (2024)
34. Liu, Z., Qi, X., Torr, P.: Global texture enhancement for fake face detection in the wild. In: *CVPR* (2020)
35. Lu, Z., Huang, D., Bai, L., Qu, J., Wu, C., Liu, X., Ouyang, W.: Seeing is not always believing: Benchmarking human and model perception of ai-generated images. In: *Thirty-seventh Conference on Neural Information Processing Systems Datasets and Benchmarks Track* (2023)
36. Midjourney: <https://www.midjourney.com> (2024)

37. Mirza, M., Osindero, S.: Conditional generative adversarial nets. In: Advances in Neural Information Processing Systems (NIPS) (2014)
38. Nichol, A., Dhariwal, P., Ramesh, A., Shyam, P., Mishkin, P., McGrew, B., Sutskever, I., Chen, M.: Glide: Towards photorealistic image generation and editing with text-guided diffusion models. In: ICML (2021)
39. Ojha, U., Li, Y., Lee, Y.J.: Towards universal fake image detectors that generalize across generative models. In: CVPR. pp. 24480–24489 (2023)
40. Park, T., Liu, M.Y., Wang, T.C., Zhu, J.Y.: Semantic image synthesis with spatially-adaptive normalization. In: CVPR (2019)
41. Podell, D., English, Z., Lacey, K., Blattmann, A., Dockhorn, T., Müller, J., Penna, J., Rombach, R.: Sdxl: Improving latent diffusion models for high-resolution image synthesis. arXiv preprint arXiv:2307.01952 (2023)
42. Qian, Y., Yin, G., Sheng, L., Chen, Z., Shao, J.: Thinking in frequency: Face forgery detection by mining frequency-aware clues. In: ECCV (2020)
43. Radford, A., Kim, J., Hallacy, C., Ramesh, A., Goh, G., Agarwal, S., Sastry, G., Askell, A., Mishkin, P., et al., J.C.: Learning transferable visual models from natural language supervision. In: ICML. pp. 8748–8763 (2021)
44. Radford, A., Metz, L., Chintala, S.: Unsupervised representation learning with deep convolutional generative adversarial networks. In: ICLR (2016)
45. Ramesh, A., Dhariwal, P., Nichol, A., Chu, C., Chen, M.: Hierarchical text-conditional image generation with clip latents. arXiv preprint arXiv:2204.06125 (2022)
46. Rombach, R., Blattmann, A., Lorenz, D., Esser, P., Ommer, B.: High-resolution image synthesis with latent diffusion models. In: Proceedings of the IEEE/CVF Conference on Computer Vision and Pattern Recognition. pp. 10684–10695 (2022)
47. Rombach, R., Blattmann, A., Lorenz, D., Esser, P., Ommer, B.: Stable diffusion (2022)
48. Sha, Z., Li, Z., Yu, N., Zhang, Y.: Defake: Detection and attribution of fake images generated by text-to-image diffusion models. In: ACM SIGSAC Conference on Computer and Communications Security. pp. 3418–3432 (2023)
49. Song, Y., Sohl-Dickstein, J., Kingma, D.P., Kumar, A., Ermon, S., Poole, B.: Score-based generative modeling through stochastic differential equations. In: Proceedings of the International Conference on Learning Representations (2021)
50. Wang, S.Y., Wang, O., Zhang, R., Owens, A., Efros, A.A.: Cnn-generated images are surprisingly easy to spot... for now. In: CVPR. pp. 8695–8704 (2020)
51. Wang, Z., She, Q., Ward, T.: Generative adversarial networks in computer vision: A survey and taxonomy. ACM Computing Surveys (2021)
52. Which face is real?: <http://www.whichfaceisreal.com>
53. Yang, L., Zhang, Z., Song, Y., Hong, S., Xu, R., Zhao, Y., Zhang, W., Cui, B., Yang, M.H.: Diffusion models: A comprehensive survey of methods and applications. ACM Computing Surveys **56**, 1–39 (2023)
54. Yu, F., Zhang, Y., Song, S., Seff, A., Xiao, J.: Lsun: Construction of a large-scale image dataset using deep learning with humans in the loop. arXiv preprint arXiv:1506.03365 (2015)
55. Zhong, N., Xu, Y., Li, S., Qian, Z., Zhang, X.: Patchcraft: Exploring texture patch for efficient ai-generated image detection. arXiv preprint arXiv:2311.12397 (2024)
56. Zhu, J.Y., Park, T., Isola, P., Efros, A.A.: Unpaired image-to-image translation using cycle-consistent adversarial networks. In: ICCV (2017)